

# An integrated label-free cell-based biosensor for simultaneously monitoring of cellular physiology multiparameter *in vitro*

Ning Hu · Jie Zhou · Kaiqi Su · Diming Zhang · Lidan Xiao · Tianxing Wang · Ping Wang

Published online: 22 February 2013  
© Springer Science+Business Media New York 2013

**Abstract** The study presented a novel integrated cell-based biosensor with light-addressable potentiometric sensor (LAPS) and electrical cell-substrate impedance sensor (ECIS). The integrated cell-based biosensor was fabricated in order to monitor the cellular metabolism and growth status by LAPS and ECIS. Moreover, the specific instrument was established for controlling the detection processes. Sensor test and cell experiments were carried out to determine the performance of integrated sensor. The result showed that integrated biosensor can monitor the change of cell electrical impedance and extracellular acidification simultaneously which can be used for drug evaluation by monitoring cell growth status (e.g. cell number, adhesion, and morphology) and cell energy metabolism status (e.g. extracellular acidification) in real time. With the development of sensor technology, the integrated cell-based biosensor will be a utility platform to study the mechanism of cellular metabolism and *in vitro* drug analysis.

**Keywords** Integrated cell-based biosensor · Light-addressable potentiometric sensor (LAPS) · Electrical cell-substrate impedance sensor (ECIS) · Cellular growth and metabolism · *In vitro* drug analysis

N. Hu · J. Zhou · K. Su · D. Zhang · L. Xiao · T. Wang · P. Wang (✉)

Biosensor National Special Laboratory, Key Laboratory for Biomedical Engineering of Education Ministry, Department of Biomedical Engineering, Zhejiang University, Hangzhou 310027, People's Republic of China  
e-mail: cnpwang@zju.edu.cn

T. Wang  
ACEA Bio (Hangzhou) Co., LTD, West Lake Technical & Economic Park, Hangzhou 310030, People's Republic of China

## 1 Introduction

For a living cell, thousands of biological reactions happen in a complicated network *in vivo*. Most of reactions depend on the energy, and then the cascade reactions are tightly coupled. Energy metabolism is a common reaction in cellular metabolism, which provides energy adenosine triphosphate (ATP) for the normal physiological activities of cells. (Frauwirth et al. 2002; Kim et al. 2006; Kishi et al. 1999; Mandel 1986) Besides, the cells release the acidic products to maintain the homeostasis of intercellular environment (Glunde et al. 2003; Gomes et al. 2001; Neve et al. 1992; Owicki and Wallace Parce 1992). Light-addressable potentiometric sensor (LAPS) is an electrochemical sensor for pH measurement (Wagner et al. 2006; Wagner et al. 2007; Schöning et al. 2005; Miyamoto et al. 2009; Miyamoto et al. 2011). Taking these advantages of LAPS into consideration, it is possible to monitor the extracellular acidification of cell (Hafeman et al. 1988; Owicki et al. 1994; McConnell et al. 1992; Hafner 2000).

Moreover, cells adhesion for proliferation is always the first step in a cell-based experiment (Perillo et al. 1998; Sung et al. 1998; Lakard et al. 2004). And electrical cell-substrate impedance sensor (ECIS) is another utility biosensor to monitor cell electrical impedance during the whole cell experiment. Cell electrical impedance reflects the characteristics of cells and electrode, such as cell number, cell adhesion, and cell morphology on planar electrodes (Giaever et al. 1986; Xiao et al. 2002; Wang et al. 2008; Ehret et al. 1998; Zou et al. 2007). Interdigital electrode is a typical type of ECIS, which has a higher sensitivity for surface impedance change compared to monopolar electrodes (Pliquett et al. 2010). Both LAPS and ECIS have emerged as the most important and interesting label-free

technology for *in vitro* cell-based assays. Integrating LAPS and ECIS on a single chip facilitates to detect two types of signals simultaneously. Generally, ECIS signals reflect the cell status such as number of cells covering the electrodes, the strength of cells attachment, and the morphology of cells, while LAPS signals reflect the energy metabolism status which is described by extracellular acidification. So, the cell growth status and energy metabolism status can be monitored simultaneously during each stage of experiment. From the simultaneous signals, the cell growth status can be monitored under drug effect in a long time, and the energy metabolism status can be reflected immediately after the drug action in a short time.

In this study, an integrated cell-based biosensor with LAPS and ECIS was designed to realize the multiparameter cell physiology detection. The fabrication processes were presented and the specific detection instrument was established. The performance of LAPS for the cell metabolism and the ECIS for the cell status were determined by the basic characteristic test experiments and

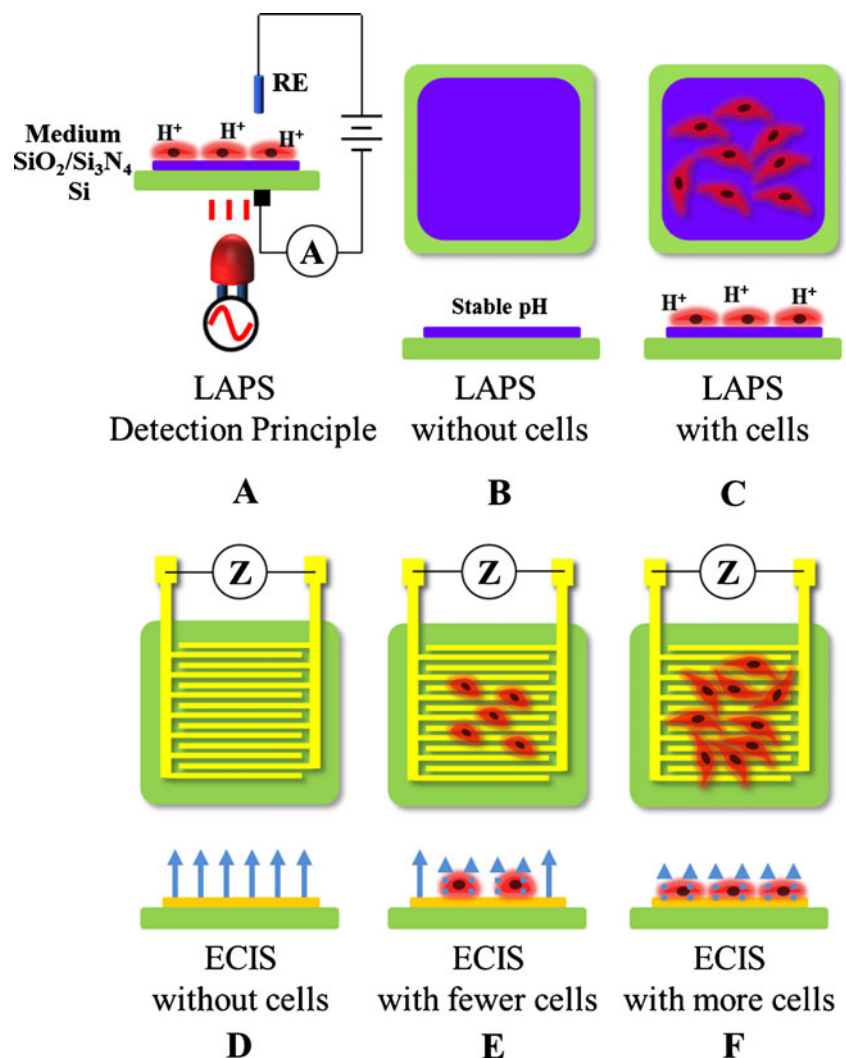
the cell drug experiments. All the details will be discussed in the following sections.

## 2 Sensor working principle

### 2.1 LAPS for cellular metabolism

LAPS can sense the small pH variation with an electrolyte/insulator/semiconductor (EIS) structure. Schematic of LAPS system is displayed in Fig. 1a. The EIS structure corresponds to medium,  $\text{SiO}_2/\text{Si}_3\text{N}_4$ , and Si, respectively. If a bias voltage is applied on the reference electrode (RE), a depletion layer is formed in the silicon which contacts with the insulator layer. By a frequency-modulated infrared light driving, LAPS generates an AC photocurrent with same frequency. This photocurrent corresponds to a hole-electron pair creation by radiation absorption from the LED. The photocurrent which is related to  $\text{H}^+$ -induced surface potential outflows from the aluminum layer. (Owicki et al. 1994; Hafeman et al. 1988;

**Fig. 1** Detection principle of light-addressable potentiometric sensor (LAPS) and electrical cell-substrate impedance sensor (ECIS) for the cellular status. **a** Schematic of LAPS detection system. **b** LAPS without cells. **c** LAPS with cells. **d** Schematic of ECIS detection system. **e** ECIS with fewer cells. **f** ECIS with more cells



Hafner 2000; McConnell et al. 1992) Insulating layer plays a significant role in pH detection, which forms the depletion with Si and interacts with  $H^+$  in the solution to form a group of silanol (Si-OH) and silamine (Si-NH<sub>2</sub>). Consequently,  $H^+$  concentration in the solution can affect the surface potential of LAPS.

Cellular metabolism begins with uptake of oxygen, glucose, and other nutrients. Cells degrade these nutrients to generate the energy ATP and finally secrete the acidic products. In aerobic condition, glucose is converted into CO<sub>2</sub> with energy by the pathway of glycolysis, citric acid cycle and oxidative phosphorylation. In anaerobic conditions, glucose is converted into lactate with energy by the pathway of the glycolysis combining lactate dehydrogenase (Kishi et al. 1999). CO<sub>2</sub> and lactic acid are hydrolyzed to HCO<sub>3</sub><sup>-</sup>/H<sup>+</sup> and lactate/H<sup>+</sup> in the cell, respectively. And these acidic products can also pass through the plasma membrane in the form of an unhydrolyzed state and are hydrolyzed outside the cell (McConnell et al. 1992), which acidify the extracellular microenvironment (Fig. 1c). Cells metabolize at a stable level under the normal condition, which is defined as the basal activity. The extracellular acidification can be disturbed by many factors, such as nutrients supplement, receptor-ligand interaction, and drug stimulation, etc. The change of factors result in fluctuation of cellular metabolism, which can be reflected by the variation of extracellular acidification rate. The pH variation can be detected by LAPS in the real time.

## 2.2 ECIS for cellular status

Electrical cell-substrate impedance sensor (ECIS) is one of the electrochemical techniques that can be applied to monitor cell adhesion, proliferation, and migration in real time. Figure 1 also shows a schematic of the ECIS system. The interdigital electrodes (IDEs) are the typical ECIS electrode for impedance sensing. If there is no cell on the ECIS, the ion current can flow freely from electrode to solution. While cells grow and adhere on the ECIS surface, Cells in contact with electrodes affect the local ionic environment at the electrode/solution interface, leading to an increase in electrical impedance. The more cells attach to the electrodes induce the increase of electrical impedance. Impedance also changes with respect to the quality of the cell interaction with electrodes. Increased cell adhesion or spreading produces a large change in impedance.

Electrical cell-substrate impedance is displayed as an arbitrary unit referred to as cell index (CI), which is a ratio of the change in impedance to background impedance. The mathematical equation is  $CI=(Z_X-Z_0)/Z_0$ . Where  $Z_X$  is the impedance with cell growth on the ECIS,  $Z_0$  is background impedance without cell on the ECIS. CI can range from 0 to 6 which depends on cell growth status and electrode

characteristics. CI reflects cell viability, cell number, cell morphology, and cell adhesion which are the relative change in measured impedance, accurately measuring cell status and changes in cell status. When cells are not present or are not adhering to the electrodes (Fig. 1d), the CI value is zero. CI values are larger when more cells attach to the electrodes (Fig. 1e), under the same physiological conditions, CI values are a quantitative measure of the number of cells on the ECIS. Change in cell status, such as cell morphology, cell adhesion, or cell viability produces a measurable, reproducible change in CI values.

## 3 Experimental and method

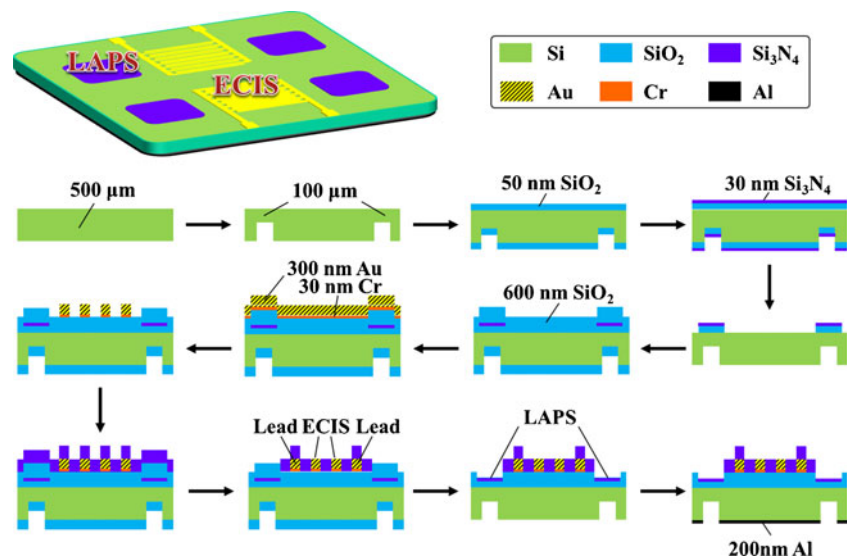
### 3.1 Integrated sensor fabrication

Integrated sensor included both LAPS and ECIS fabrication, which are different from the each sensor fabrication (Xiao et al. 2010; Xu et al. 2005; Yoshinobu et al. 2004; Haas et al. 2010). The full view and fabrication processes of the integrated sensor were presented in the Fig. 2. Taking the LAPS into consideration, the N-type silicon wafers (500 μm thick and 4 inches in diameter) with specific resistance of 10 Ω•cm and orientation index of crystal orientation  $\langle 1\ 0\ 0 \rangle$  were selected for the integrated chip. As illustrated in Fig. 2, the silicon wafer was partially grinded from 500 μm to 100 μm to increase the LAPS sensitivity. After RCA cleaning process, the silicon surface was insulated with a layer of 50 nm SiO<sub>2</sub> by thermally oxidation at 1000 °C. Then a thin layer of 30 nm Si<sub>3</sub>N<sub>4</sub> was deposited by low pressure chemical vapor deposition (LPCVD) as a sensitive and protective layer on the upper side of SiO<sub>2</sub>. And then a SiO<sub>2</sub> and Si<sub>3</sub>N<sub>4</sub> layer was partially removed through etching after photolithography. Thus the LAPS region was formed on the chip.

Before the fabrication of ECIS, a thick layer of 600 nm SiO<sub>2</sub> was deposited on the sensor surface by plasma enhanced chemical vapor deposition (PECVD) as the insulator layer between the metal electrode and the silicon substrate, and as a protective layer for the LAPS surface. The 300 nm Au and 30 nm Cr were used as metal electrodes. Cr can enhance the adhesion of Au and SiO<sub>2</sub>. Subsequently, the electrode and lead patterns of ECIS were formed through etching after photolithography. 800 nm Si<sub>3</sub>N<sub>4</sub> was deposited by LPCVD in order to insulate the lead of ECIS from the external solution. And then Si<sub>3</sub>N<sub>4</sub> on the electrode of ECIS was removed. Also, the thick SiO<sub>2</sub> protective layer on the LAPS was removed. Finally, the 200 nm Al was evaporated on the backside of the silicon chip to form an ohmic contact.

The thicknesses of SiO<sub>2</sub> layer and the Si<sub>3</sub>N<sub>4</sub> layer on LAPS and Cr layer and Au layer on ECIS of integrated sensor was similar to individual LAPS and ECIS sensor.

**Fig. 2** Schematic of integrated sensor including the LAPS and ECIS. Full view of integrated sensor (on the top) and the fabrication processes (on the bottom)



One challenge of the integrated sensor as compared to individual LAPS and ECIS sensor was 600 nm SiO<sub>2</sub> and 800 nm Si<sub>3</sub>N<sub>4</sub> as the insulator layers, which ensured the ECIS function without interference by the Si substrate and solution. Another improvement of the integrated sensor was LAPS fabrication. The silicon wafer was partially grinded from 500 μm to 100 μm to increase the LAPS sensitivity by reducing the infrared light attenuation.

### 3.2 Experimental setup

The sensor unit consisted of three parts, culture chamber, integrated sensor, and LED array as shown in Fig. 3a and c. The culture chamber was fixed onto the integrated sensor with inlet and outlet for cell culture and flow analysis. Integrated sensor monitored the cellular metabolism and growth status. The LED array was fixed under the integrated sensor for LAPS detection. All of the ports were connected with a printed circuit board (PCB) board. The detection signals of the LAPS and ECIS were both AC current, so main modules of the analysis instrument can be similar. E.g. the signal generator of LAPS can be used to drive the ECIS with the same frequency 10 kHz and the detection modules was exactly same including the potentiostat, lock-in amplifier, AD convertor. The relay-based multiplexer played a significant role in controlling the LAPS and ECIS detection. All the processes can be carried out orderly by the MCU. The whole detection system was shown in Fig. 3b and d.

### 3.3 Cell culture

Renal cells have active metabolism in the neonatal Sprague Dawley (SD) rats which facilitated to carry out the energy metabolism experiment, and renal cells can be cultured

easily. So the renal cells were employed for the experimental analysis. These cells were derived from the 3 to 5 days old neonatal SD rats.  $5 \times 10^5$  cells/ml were cultured on the integrated chip for 24 h under standard conditions (37 °C, 5 % CO<sub>2</sub>, RPMI cell culture medium supplemented with 10 % fetal bovine serum, 2 g/l bicarbonate, 100 IU/ml penicillin, 100 μg/ml streptomycin). In the cell experiment, the modified RPMI-1640 medium was buffered with only 1 mMPBS, and Sodium bicarbonate was excluded. But in order to keep the osmotic balance, an appropriate amount of NaCl had to be added to the medium. This low buffer capacity ensured the sensor system to detect the small pH change.

## 4 Results and discussion

### 4.1 Sensor performance determination

The performance of integrated sensor was determined before the cell experiments, especially for LAPS. Photocurrent-voltage (PV) curve was one of the most important characteristics to reflect the pH sensitivity. Figure 4a presented the PV characteristic under the different pH. The photocurrent-voltage curves shifted onto the positive from low pH to high pH, which can moves reproducibly along the voltage axis depending on the pH. The result shows that the electrolyte/insulator interphase potential was coupled onto the DC bias potential, affecting the bias potential applied on the LAPS. Conventionally, the inflection point of each PV curve was pH-dependent which was calculated by second derivative. The pH calibration curve was shown in Fig. 4b. The pH sensitivity of the LAPS was 57.7 mV/pH. PV calibration was the traditional method to test the pH performance, and pH curve was similar to a pH spectrum for the constant current detection mode that



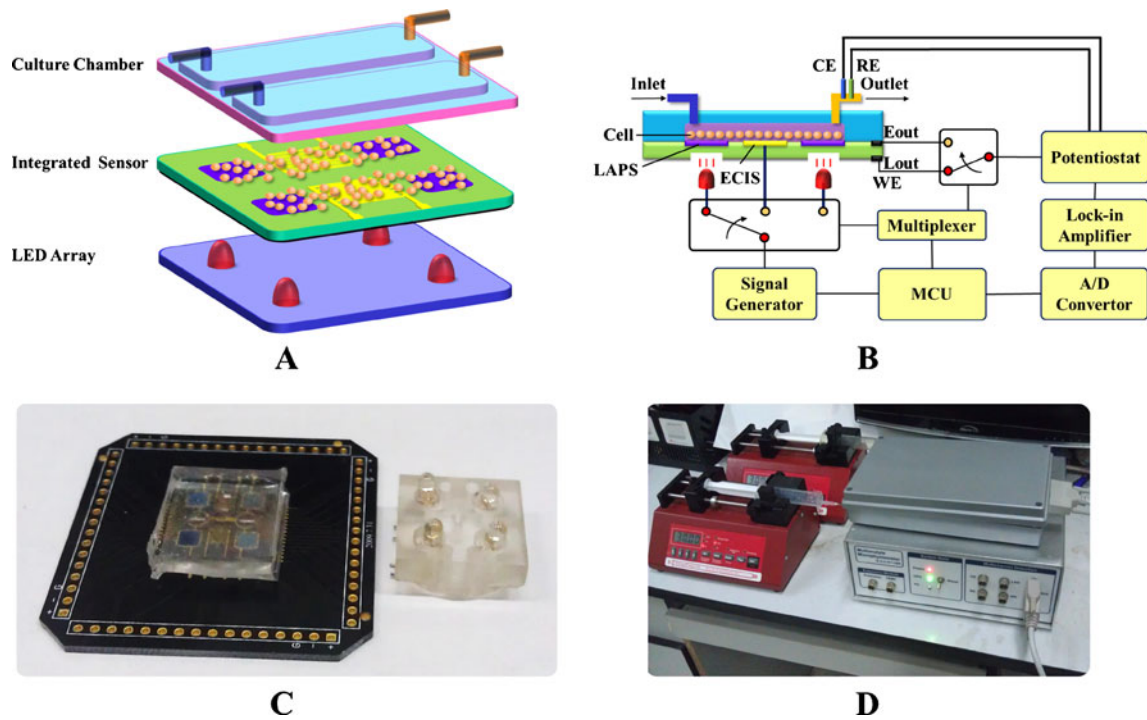


Fig. 3 Sensor unit and integrated sensor detection system. Sensor unit (a) and (c). Integrated sensor detection system (b) and (d)

reflected the characteristic under each bias voltage and each pH. Constant voltage detection mode was another method which can reflect the pH-induced variation directly. Under

this mode, the bias voltage applied on the reference electrode was constant, which was selected from the PV curve in the linear working region. The pH sensitivity was 1050 nA/pH

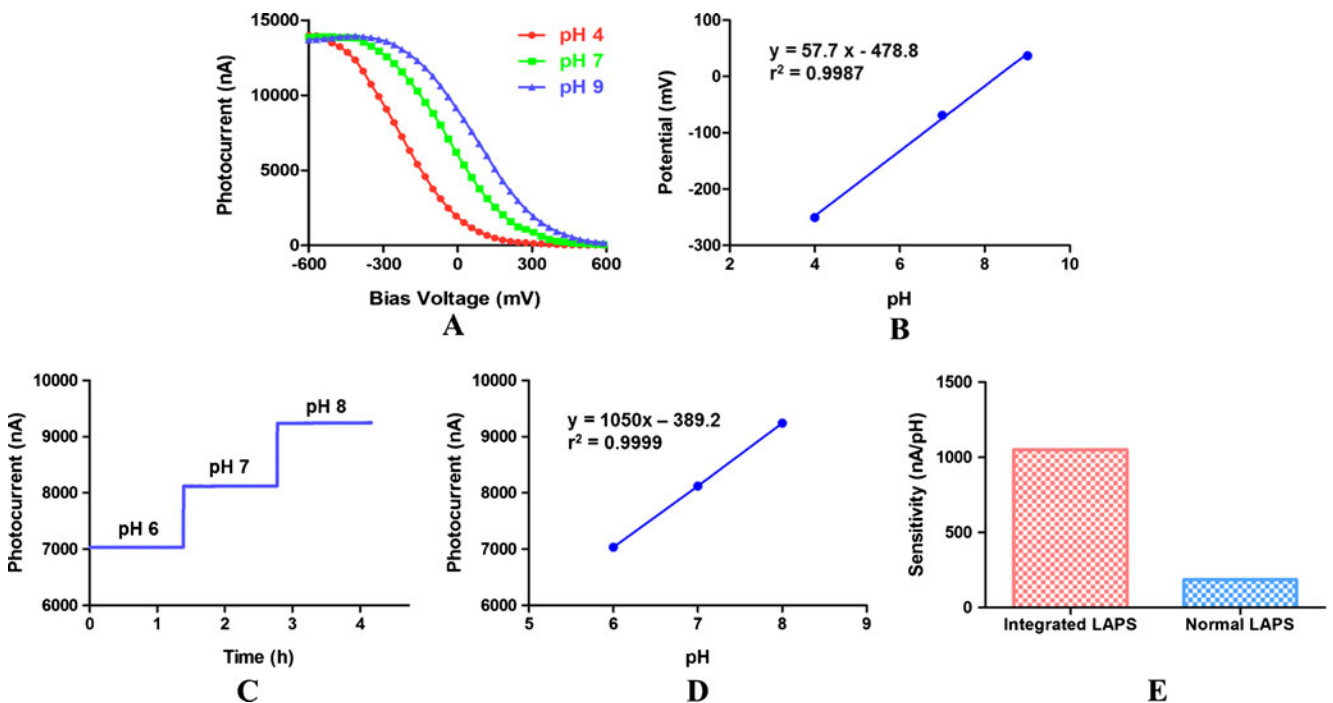


Fig. 4 Sensor performance determination. a Photocurrent-voltage characteristic curve. b Photocurrent-voltage curve pH calibration result. c Constant voltage mode characteristic curve. d Constant voltage mode pH calibration result

(integrated LAPS) *versus* 184 nA/pH (normal LAPS). (Figure 4c and d). The performance of ECIS was determined in the following cell experiments.

#### 4.2 Cell physiological status monitoring and drug analysis

The neonatal SD rat Cells were cultured on the integrated sensor in the cell incubator for 24 h. Figure 5a and b were the Wright staining cells on the ECIS region and LAPS region, respectively. After the cells were cultured on the integrated sensor, the cell experiments were carried out.

ECIS on the integrated sensor was used for impedance-based measurement which provided a holistic way to reflect cell growth status. The impedance of ECIS with cells was higher than that of ECIS without cells. After monitoring the cell status for 2.5 h, the triton was added into the culture

chamber. And the impedance of the ECIS with cells dropped significantly to a low level, while the ECIS without cells was relatively stable. (Figure 5c and e) And the cell index (CI) can be calculated based on ECIS with cells and without cells. When cells were not adhering to the ECIS electrodes, the CI value was zero. Under the same physiological conditions, CI values were larger when more cells attached to the electrodes. CI values are a quantitative measure of the number of cells. CI value drop to a low level.

Meanwhile LAPS on the integrated sensor was used for pH measurement. In order to measure the extracellular acidification rate (ECAR) continuously, the pump-off and pump-on protocol was employed. Cells released the acidic wastes to maintain the intercellular environment homeostasis. In the pump-off stage, the acidic products accumulated in the extracellular environment, so the pH dropped to a low level. While

**Fig. 5** The typical cell experiment results. **a** The neonatal SD rat renal cells cultured on the ECIS region of integrated sensor after Wright staining in 24 h later. **b** Cells cultured on LAPS region. **c** The impedance comparison of sensor with cells and without cells under triton effect. **d** Extracellular acidification response comparison of sensor with cells and without cells under triton effect. **e** Cell index corresponding to the impedance variation. **f** Extracellular acidification rate calculated by linear fit of the extracellular acidification response signals

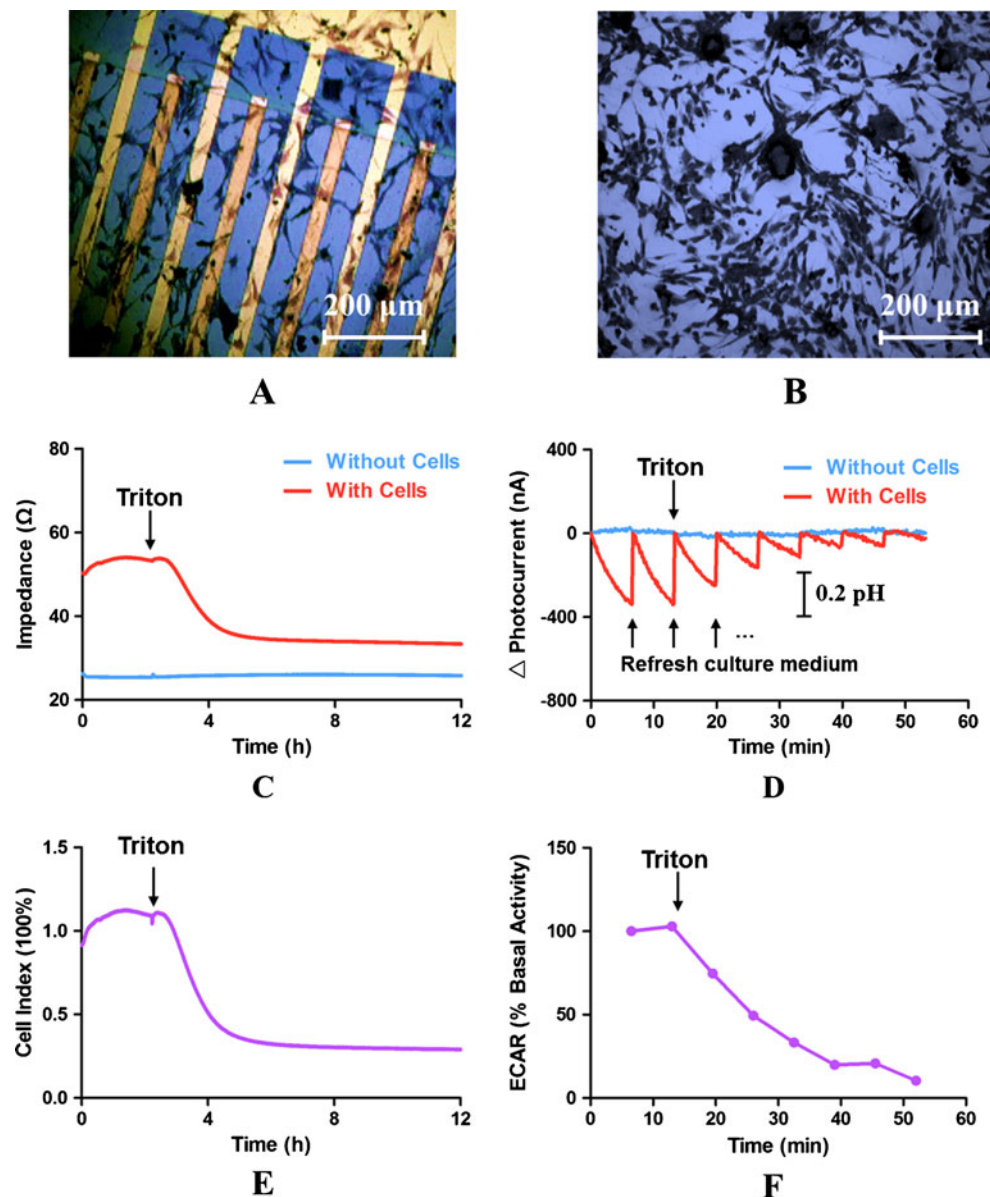
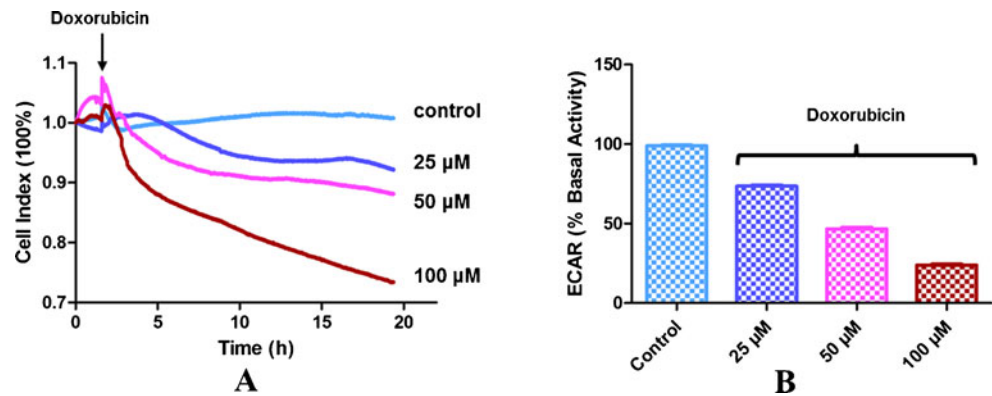


**Fig. 6** Typical cellular status and metabolism under the doxorubicin. Cell electrical impedance (a) and extracellular acidification rate (b) variation under the different condition



fresh culture medium washed the acidic products away from the chamber in the pump-on stage, and the pH recovered to the original level. The response signals of LAPS without cells have a small fluctuation which was induced by the medium injection. After the triton was added, the extracellular acidification gradually reduced. The ECAR value can be calculated by the linear fit of signals in the pump-off stage. The ECAR value of cells in the absence of triton was considered as the basal extracellular acidification rate. And other ECAR values can be compared with the basal activity. With the effect of triton, the metabolism of cell population decreased to a low level. (Figure 5d and f) Triton X-100 is a commonly used detergent in laboratories. Some applications include permeabilizing unfixed (or lightly fixed) eukaryotic cell membranes, solubilizing membrane proteins in their native state in conjunction with zwitterionic detergents such as CHAPS. And it was often used as the agent for acute cell experiments.

After the cells were cultured for 24 h, the CI values were similar at the beginning. An anti-cancer drug, doxorubicin was selected to study the harm to the renal cells in a relative low rate. And then the doxorubicin, an anti-cancer drug used in chemotherapy was added to form the control and treatment groups (25  $\mu\text{M}$ , 50  $\mu\text{M}$ , 100  $\mu\text{M}$ ). With the increase of doxorubicin concentration, CI value declined sharply. The CI was about 92 %, 88 %, and 73 % after the treatment of doxorubicin, respectively (Fig. 6a). In contrast, the CI under the treatment of 100  $\mu\text{M}$  doxorubicin showed a fast and consecutive drop in 20 h. Besides, the extracellular acidification rate decreased to 73 %, 47 %, and 24 % of the basal activity. From the ECIS impedance signals and LAPS signals, the CI gradually decreased to a low level and the extracellular acidification rate also dropped with concentration-dependence, which meant that cells growth status and energy metabolism was destroyed by doxorubicin. The peaks in experiment results were mainly induced by injecting the medium too rapidly into the sensor chamber. And the injecting medium fluctuation caused the cell status fluctuation. For more reliable cell experiment results, the injecting system needs to be improved by selecting the appropriate injecting rate and preventing the unnecessary disturbance.

Based on the results of the experiments, it can be concluded that the integrated cell-based sensor can monitor the cell status, cell metabolism and the drug-induced cytotoxicity. Compared with the *in vivo* animal experiment, cell-based biosensor reflects the drug effect in a shorter time. *In vivo* experiments use live animal. Usually, the disease animal model will be established for drug experiments, and the disease on animal will be observed day by day, which continues for days, even for months. While the cell-based biosensor is established by culturing the cells on the sensor chip and drug effect on cells can be directly reflected in minutes or hours. Moreover, the integrated sensor can reflect the cell physiological characteristic in the presence of stimulus in more ways. Intended purposes of integrated sensor are to measure cellular metabolism and cellular electrical impedance for cell physiology study and drug evaluation, and combining the improved LAPS and ECIS is the first step to develop integrated sensors. In this study, we mainly focus on determining the basic performance of integrated biosensor by calibration and drug experiments. The integrated sensor can help to reflect the cell status in more aspects with multi-parameter detection. In order to reveal more information between ECIS signals and LAPS signals, more experiments and methods should be designed to present the better performance of integrated biosensor in the further research. Thus, the integrated cell-biosensor can present the drug effect from different cell physiological status.

## 5 Conclusions

In the study, integrated biosensor was established to simultaneously detect the change of cell electrical impedance and extracellular acidification, which provided a utility drug analysis platform by monitoring and analyzing the correlation between cell growth status and cell energy metabolism status in a noninvasive and label-free way. Besides, the pH sensitivity of LAPS was improved by decreasing the silicon



substrate, which enhanced the performance of the surface potential-photocurrent conversion. On the integrated sensor, LAPS was used to detect the extracellular acidification. While ECIS reflects cell viability, cell number, cell morphology, and cell adhesion. By employing neonatal SD rat renal cells, the performance of integrated biosensor was proved for monitoring cell status and metabolism under the drug effect. With the development of sensor technology, more biosensors can be involved in one integrated chip for *in vitro* studying cells physiology.

**Acknowledgments** This work was supported by 973 Program of Ministry of Science and Technology of China (No. 2009CB320303), National Public Welfare Project of China (No. 201305010), and National Natural Science Foundation of China (No. 81027003).

## References

- R. Ehret, W. Baumann, M. Brischwein, A. Schwinde, B. Wolf, On-line control of cellular adhesion with impedance measurements using interdigitated electrode structures. *Med Biol Eng Comput* **36**, 365–370 (1998)
- K.A. Frauwirth, J.L. Riley, M.H. Harris, R.V. Parry, J.C. Rathmell, D.R. Plas, R.L. Elstrom, C.H. June, C.B. Thompson, The CD28 signaling pathway regulates glucose metabolism. *Immunity* **16**, 769–777 (2002)
- I. Giaever, Keese, C.R., Use of electric fields to monitor the dynamical aspect of cell behavior in tissue culture. *Biomedical Engineering, IEEE Transactions on* 242–247 (1986)
- K. Glunde, S.E. Guggino, M. Solaiyappan, A.P. Pathak, Y. Ichikawa, Z.M. Bhujwala, Extracellular acidification alters lysosomal trafficking in human breast cancer cells. *Neoplasia (New York, NY)* **5**, 533 (2003)
- P. Gomes, M. Vieira-Coelho, P. Soares-Da-Silva, Ouabain-insensitive acidification by dopamine in renal OK cells: primary control of the Na<sup>+</sup>/H<sup>+</sup> exchanger. *Am. J. Physiol. Regul. Integr. Comp. Physiol.* **281**, R10–R18 (2001)
- S. Haas, H.G. Jahnke, M. Glass, R. Azendorf, S. Schmidt, A.A. Robitzki, Real-time monitoring of relaxation and contractility of smooth muscle cells on a novel biohybrid chip. *Lab. Chip* **10**, 2965–2971 (2010)
- D.G. Hafeman, J.W. Parce, H.M. McConnell, Light-addressable potentiometric sensor for biochemical systems. *Science* **240**, 1182–1185 (1988)
- F. Hafner, Cytosensor<sup>®</sup> Microphysiometer: technology and recent applications. *Biosens. Bioelectron.* **15**, 149–158 (2000)
- J. Kim, I. Tchernyshyov, G.L. Semenza, C.V. Dang, HIF-1-mediated expression of pyruvate dehydrogenase kinase: a metabolic switch required for cellular adaptation to hypoxia. *Cell metabolism* **3**, 177–185 (2006)
- Y. Kishi, J. Schmelzer, J. Yao, P. Zollman, K. Nickander, H. Tritschler, P. Low, Alpha-lipoic acid: effect on glucose uptake, sorbitol pathway, and energy metabolism in experimental diabetic neuropathy. *Diabetes* **48**, 2045–2051 (1999)
- S. Lakard, G. Herlem, A. Propper, A. Kastner, G. Michel, N. Valles-Villarreal, T. Gharbi, B. Fahys, Adhesion and proliferation of cells on new polymers modified biomaterials. *Bioelectrochemistry* **62**, 19–27 (2004)
- L.J. Mandel, Energy metabolism of cellular activation, growth, and transformation. *Current Topics in Membranes Trans.* **27**, 261–291 (1986)
- H. McConnell, J. Owicki, J. Parce, D. Miller, G.T. Baxter, H. Wada, S. Pitchford, The cytosensor microphysiometer: biological applications of silicon technology. *Science* **257**, 1906–1912 (1992)
- K. Miyamoto, Y. Kuwabara, S. Kanoh, T. Yoshinobu, T. Wagner, M.J. Schöning, Chemical image scanner based on FDM-LAPS. *Sensors Actuators B: Chemical* **137**, 533–538 (2009)
- K. Miyamoto, T. Wagner, T. Yoshinobu, S. Kanoh, M.J. Schöning, Phase-mode LAPS and its application to chemical imaging. *Sensors Actuators B: Chemical* **154**, 28–32 (2011)
- K.A. Neve, M. Kozlowski, M. Rosser, Dopamine D2 receptor stimulation of Na<sup>+</sup>/H<sup>+</sup> exchange assessed by quantification of extracellular acidification. *J. Biol. Chem.* **267**, 25748–25753 (1992)
- J.C. Owicki, L.J. Bousse, D.G. Hafeman, G.L. Kirk, J.D. Olson, H.G. Wada, J.W. Parce, The light-addressable potentiometric sensor: principles and biological applications. *Annu. Rev. Biophys. Biomol. Struct.* **23**, 87–114 (1994)
- J.C. Owicki, J. Wallace Parce, Biosensors based on the energy metabolism of living cells: the physical chemistry and cell biology of extracellular acidification. *Biosens. Bioelectron.* **7**(255–272) (1992)
- N. Perillo, M.E. Marcus, L.G. Baum, Galectins: versatile modulators of cell adhesion, cell proliferation, and cell death. *J Mol Med* **76**, 402–412 (1998)
- U. Pliquet, D. Frense, M. Schönfeldt, C. Frätzer, Y. Zhang, B. Cahill, M. Metzen, A. Barthel, T. Nacke, D. Beckmann, Testing miniaturized electrodes for impedance measurements within the beta-dispersion—a practical approach. *J Elect Bioimpedance* **1**, 41–55 (2010)
- M. Schöning, T. Wagner, C. Wang, R. Otto, T. Yoshinobu, Development of a handheld 16 channel pen-type LAPS for electrochemical sensing. *Sensors Actuators B: Chemical* **108**, 808–814 (2005)
- V. Sung, J. Stubbs Iii, L. Fisher, A. Aaron, E. Thompson, Bone sialoprotein supports breast cancer cell adhesion proliferation and migration through differential usage of the  $\alpha v \beta 3$  and  $\alpha v \beta 5$  integrins. *J. Cell. Physiol.* **176**, 482–494 (1998)
- T. Wagner, R. Molina, T. Yoshinobu, J.P. Kloock, M. Biselli, M. Canzoneri, T. Schnitzler, M.J. Schöning, Handheld multi-channel LAPS device as a transducer platform for possible biological and chemical multi-sensor applications. *Electrochim. Acta* **53**, 305–311 (2007)
- T. Wagner, C. Rao, J. Kloock, T. Yoshinobu, R. Otto, M. Keusgen, M. Schöning, “LAPS Card”—A novel chip card-based light-addressable potentiometric sensor (LAPS). *Sensors Actuators B: Chemical* **118**, 33–40 (2006)
- L. Wang, J. Zhu, C. Deng, W. Xing, J. Cheng, An automatic and quantitative on-chip cell migration assay using self-assembled monolayers combined with real-time cellular impedance sensing. *Lab Chip* **8**, 872–878 (2008)
- C. Xiao, B. Lachance, G. Sunahara, J.H.T. Luong, Assessment of cytotoxicity using electric cell-substrate impedance sensing: concentration and time response function approach. *Anal. Chem.* **74**, 5748–5753 (2002)
- L. Xiao, Z. Hu, W. Zhang, C. Wu, H. Yu, P. Wang, Evaluation of doxorubicin toxicity on cardiomyocytes using a dual functional extracellular biochip. *Biosens. Bioelectron.* **26**, 1493–1499 (2010)
- G. Xu, X. Ye, L. Qin, Y. Xu, Y. Li, R. Li, P. Wang, Cell-based biosensors based on light-addressable potentiometric sensors for single cell monitoring. *Biosens. Bioelectron.* **20**, 1757–1763 (2005)
- T. Yoshinobu, M.J. Schöning, F. Finger, W. Moritz, H. Iwasaki, Fabrication of thin-film LAPS with amorphous silicon. *Sensors* **4**, 163–169 (2004)
- Z. Zou, J. Kai, M.J. Rust, J. Han, C.H. Ahn, Functionalized nano interdigitated electrodes arrays on polymer with integrated microfluidics for direct bio-affinity sensing using impedimetric measurement. *Sensors Actuators A: Physical* **136**, 518–526 (2007)